Microstructure Evolution and Mechanical Properties of Cold Hearth Furnace Melted TC1 Titanium Alloy During Rolling - Postprint

Authors: Chang Hai, Liu Mengying, Wang Ning, Feng Qiang, Xu Feng, Xu Zhengfang, Yang Zhao, Gan Weimin

Date: 2016-11-04T00:00:00+00:00

Abstract

Plasma cold hearth furnaces are widely employed for melting aerospace titanium alloys owing to the high purity of the resulting ingots. In China, industrial-scale plasma cold hearth furnace melting of titanium alloys remains in its nascent stage, necessitating urgent research into melting parameters and subsequent thermomechanical processing of the ingots. This study investigates TC1 titanium alloy produced via industrial-scale plasma cold hearth furnace melting, integrating actual production workflows and employing neutron diffraction technique to examine the influence of different rolling processes on the microstructural and property evolution of TC1 rolled sheets, thereby elucidating the microstructure-mechanical property relationship. The results demonstrate that the as-cast microstructure of the cold hearth furnace ingot exhibits a Widmanstätten structure. Following rolling, the α colonies become distorted and fragmented. The alignment of deformed α phase along the rolling direction is more pronounced in unidirectional rolling than in cross rolling. Upon annealing, the deformed α phase in the sheets undergoes spheroidization. Both unidirectional and cross rolled sheets display a prismatic texture, which accounts for the significantly higher transverse yield strength relative to the rolling direction yield strength.

Full Text

Microstructure Evolution and Mechanical Properties of TC1 Alloy Fabricated by Plasma Arc Cold Hearth Melting During Rolling Process

LIU Mengying[1], **CHANG Hai**[1], **XU Feng**[2], **XU Zhengfang**[2], **YANG Zhao**[2], **WANG Ning**[2], **GAN Weimin**[3], **FENG Qiang**[1,4]

[1] National Center for Materials Service Safety, University of Science and Technology Beijing, Beijing 100083
[2] Baosteel Special Metals Co., Ltd., Shanghai 200940
[3] Helmholtz-Zentrum Geesthacht, Out Station at FRM2, Garching, Germany, 85747
[4] State Key Laboratory for Advanced Metals and Materials, University of Science and Technology Beijing, Beijing 100083

Abstract: Plasma arc cold hearth melting (PAM) is an effective technology for producing high-purity titanium alloy ingots widely used in aerospace applications. However, PAM development in China remains in its initial stages, necessitating investigation of both melting parameters and subsequent thermomechanical processing of PAM-fabricated ingots. In this study, TC1 alloy ingots produced by PAM were cogged at the β transus temperature, then rolled using unidirectional and cross rolling processes in the α+β phase field. The typical Widmanstätten structure of the as-cast ingots transformed to a refined β-processed morphology after cogging, with α phases forming in smaller colonies of lamellae. Following α+β rolling, the α colonies became distorted and the α laths rearranged along the rolling direction, though cross rolling produced weaker directionality. Both unidirectional and cross rolled sheets exhibited typical prismatic texture. After annealing below the β transus temperature, the α phases transformed to an equiaxed morphology. The transverse yield strength of the sheets was significantly higher than the rolling direction yield strength, attributable to the strong prismatic texture introduced by hot rolling.

Keywords: plasma arc cold hearth melting; TC1 alloy; hot rolling; microstructure; texture; mechanical properties

Introduction

Titanium alloys are widely used in aerospace applications due to their high specific strength, excellent high-temperature properties, and outstanding corrosion resistance. Titanium is a highly reactive metal that readily reacts with many elements at melting temperatures, including various oxide refractory materials. Consequently, titanium melting must be conducted in vacuum or inert gas environments. Additionally, the use of water-cooled copper crucible chillers enables safe solidification of titanium. From an economic perspective, vacuum arc remelting has become the primary method for titanium ingot production. However, due to its short high-temperature holding time and insufficient melting temperature, this method cannot completely eliminate solidification defects such as inclusions and chemical segregation. In the 1980s, the United States developed a novel titanium alloy melting technology—cold hearth melting. Cold hearth melting is categorized into electron beam cold hearth melting and plasma arc cold hearth melting (PAM), emerging from the urgent demand for high-purity titanium alloys in aviation applications. During cold hearth melting, inclusions have sufficient time to be melted by the extremely high temperature or sink to the bottom of the hearth without entering the molten pool, thereby significantly

eliminating both high-density and low-density inclusions in titanium alloys and effectively improving chemical segregation in ingots.

Currently, international research reports on cold hearth melting of titanium alloys are scarce, and studies on subsequent thermomechanical processing of cold hearth-melted titanium alloys are even rarer. Industrial application of PAM for titanium alloys in China remains in its infancy, with limited reporting on the technological development status, and exploration of subsequent thermomechanical processing parameters for PAM titanium ingots is particularly limited. This study investigates industrial-scale PAM melting of titanium alloys and product development.

Titanium alloy microstructure is strongly influenced by thermomechanical processing parameters. Processing parameters including deformation temperature, strain rate, and cooling rate can all lead to microstructural changes, primarily affecting α/β phase morphology, α colony size, and volume fraction of equiaxed α. Processing parameters also significantly influence the type and intensity of texture in titanium alloys. Generally, the main texture types formed during titanium alloy processing include prismatic, basal, and pyramidal textures. Texture intensity is primarily determined by the degree of deformation and rolling mode. Both microstructure and texture subsequently determine the mechanical properties of titanium alloy products.

Given the current state of PAM development in China, this study investigates TC1 titanium alloy ingots produced by PAM at Baosteel Special Metals Co., Ltd. Using neutron diffraction technology, we examine the evolution of microstructure and texture during rolling of TC1 sheets and discuss the influence of thermomechanical processing on microstructure and properties, aiming to provide theoretical guidance and experimental basis for subsequent thermomechanical processing of PAM-melted TC1 titanium alloys.

Experimental

The TC1 titanium alloy ingots used in this study were produced by PAM with dimensions of 1550 mm × 750 mm × 330 mm. The nominal composition of TC1 titanium alloy is Ti-2Al-1.5Mn, with detailed chemical composition (mass fraction, %) of Al 1.0–2.5, Mn 0.7–2.0, Fe $\leq$ 0.3, C $\leq$ 0.1, N $\leq$ 0.05, H $\leq$ 0.12, O $\leq$ 0.15, and Ti balance.

A 36 mm thick slab was cut from the core of the PAM TC1 alloy ingot as the starting material for rolling deformation. The ingot was held in the β phase field, then breakdown rolled at the transus temperature. The rolled blank was subsequently reheated to the $\alpha+\beta$ two-phase region and rolled to a final sheet thickness of 3 mm. Two-phase region rolling processes included unidirectional rolling (UR) and cross rolling (CR). Unidirectional rolling maintained the initial rolling direction throughout all passes until completion. Cross rolling involved rotating the sheet 90° relative to the initial pass direction, performing another 90° rotation, and maintaining this direction for subsequent passes. No inter-pass

annealing was performed during rolling. To investigate the effects of post-rolling annealing on microstructure and properties, 3 mm sheets from both rolling processes were annealed at 750 °C for 30 min and air-cooled.

Texture measurement samples measuring 24 mm × 14 mm × 2 mm were cut from sheets processed by both rolling methods. After mechanical grinding and polishing, macro-texture measurements were conducted using the STRESS-SPEC thermal neutron diffractometer. During texture measurement, the incident thermal neutron beam had a wavelength of 0.174 nm and a diameter of 25 mm, completely covering the entire sample. Complete pole figure measurements were performed on the (0002), (MATH_0), and (MATH_1) planes. Compared with conventional X-ray diffraction, neutron beams possess strong penetration capability, enabling detection of grain orientations throughout the bulk sample, and neutron diffraction can achieve α angles up to 90° using both reflection and transmission methods, allowing acquisition of complete pole figure data.

Room temperature tensile properties of sheets processed by both rolling methods and subsequent annealing were tested using an MTS 810 testing machine at a strain rate of 0.0017 s^{-1}. Tensile specimen dimensions are shown in Figure 1a [FIGURE:1]. During testing, tensile samples were cut and tested along both the rolling direction (RD) and transverse direction (TD) of the sheets, with direction schematics shown in Figure 1b.

Metallographic specimens were prepared by mechanical grinding and electrolytic polishing, then etched with Kroll's reagent (87 mL H_2O + 10 mL HNO_3 + 3 mL HF). Microstructures were observed using an AXIO IMAGER M2m optical microscope (OM). Observations were made on both the rolling plane (RD-TD plane) and longitudinal section (RD-ND plane) of the rolled sheets.

Results

2.1 Microstructure

Figure 2 [FIGURE:2] shows typical as-cast OM images from the core of the TC1 alloy ingot produced by PAM. The low-magnification image reveals a Widmanstätten structure (Figure 2a). The prior β grain size is approximately 8 mm, with coarse α colonies forming within the original β grains. α colony sizes are non-uniform, with large colonies reaching 4 mm and some small colonies approximately 50 m. The α colonies exhibit distinct orientations, with different orientations present in adjacent β grains.

Figure 2b presents a high-magnification OM image of the as-cast microstructure, showing that each α colony consists of nearly parallel α lamellae with β phase located between the lamellae. The lamellae thickness is approximately 2 m. Additionally, primary α phase rims are observed along prior β grain boundaries.

After breakdown rolling, both the rolling plane and longitudinal section of the sheet exhibit transformed β microstructure, with the rolling plane OM image

shown in Figure 3 [FIGURE:3]. The image reveals interwoven α colonies with different orientations. Colony size is significantly reduced from the millimeter scale in the as-cast condition to approximately 400 m, with small colonies only a few micrometers in size. Prior β grain boundaries remain visible, though primary α phase rims have dissolved. Figure 3b shows a high-magnification image of the interwoven α colonies. Compared with the as-cast structure (Figure 2), the α lamellae are more closely packed after breakdown rolling, with lamellae thickness significantly reduced to approximately 0.7 m.

Figure 4 [FIGURE:4] shows typical OM images on the rolling plane and longitudinal section of TC1 sheets after unidirectional and cross rolling. After two-phase region rolling deformation, the α colonies become distorted and fragmented, with prior β grain boundaries no longer distinguishable. Differences are observed between rolling plane and longitudinal section microstructures.

After unidirectional rolling, α phase on the rolling plane aligns along the rolling direction (Figure 4a). After cross rolling, α colonies on the rolling plane are more thoroughly fragmented, with less pronounced directionality compared to unidirectional rolling (Figure 4c). Longitudinal section microstructures are similar for both processes, with α phase distributed in bands along the deformation direction and distinct flow lines visible. At high magnification, both show elongated deformed α phase (Figures 4b and d).

Figure 5 [FIGURE:5] shows typical OM images on the rolling plane and longitudinal section after annealing at 750 °C for 30 min and air cooling for both rolling processes. Figures 5a and c reveal that after annealing, both unidirectional and cross rolled sheets exhibit equiaxed α phase on the rolling plane, with β phase distributed around the α phase. The unidirectional rolled sample shows some directionality in lamellar α phase in most regions (Figure 5a [FIGURE:5]). Longitudinal section microstructures are similar for both processes, consisting of mixed equiaxed and elongated α phases (Figures 5b and d).

2.2 Macro-texture Evolution

Figure 6

shows complete pole figures of α-phase (0002), (MATH_2), and (MATH_3) planes measured by neutron diffraction after breakdown rolling. Figure 6a indicates that after breakdown rolling, α-phase (0002) plane normals are primarily parallel to the TD direction, with some distribution in the ND direction and positions deviating approximately 45° from both RD and TD. Figure 6b shows that α-phase (MATH_4) plane normals are mainly parallel to the ND direction and deviated toward RD. Figure 6c presents the (MATH_5) pole figure, which is similar to the (MATH_6) plane, with (MATH_7) plane normals primarily located within a range deviating approximately 5° from ND toward RD.

Figure 7 [FIGURE:7] shows complete pole figures of α-phase (0002),

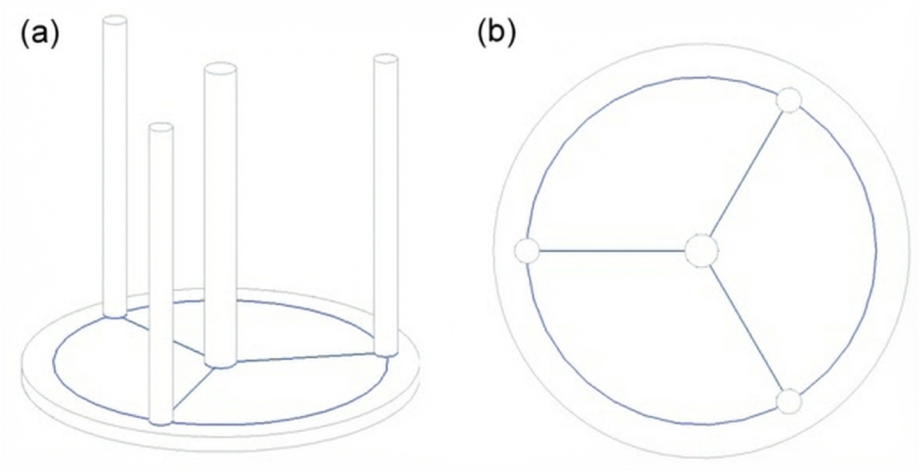

Figure 1: Figure 6

(MATH_8), and (MATH_9) planes after unidirectional and cross rolling. Figure 7a reveals that for unidirectional rolling, α-phase (0002) plane normals are primarily parallel to the TD direction with a pole intensity of 6.8. Figure 7b indicates that (MATH_{10}) plane normals are distributed along the RD direction and positions deviating approximately 60° from ND toward RD, with a small number of grains having (MATH_{11}) plane normals parallel to the ND direction. Figure 7c shows that (MATH_{12}) plane normals are mainly distributed approximately 30° from ND toward RD and along the RD direction. Figures 7a–c demonstrate that unidirectional rolling produces primarily prismatic texture characteristics. The (0002) pole figure for cross rolled sheet shows poles similarly located in the TD direction with an intensity of 5.6 (Figure 7d). Figure 7e indicates that (MATH_{13}) plane normals are mainly distributed approximately 30° from ND toward RD and along the RD direction. Figure 7f shows that (MATH_{14}) plane normals are primarily located approximately 60° from ND toward RD, with a small number of grains having (MATH_{15}) plane normals parallel to the ND direction. Similar to unidirectional rolling, cross rolled sheets also exhibit prismatic texture characteristics, though with weaker texture intensity than unidirectional rolling (Figures 7d–f).

2.3 Room Temperature Properties

Room temperature tensile properties of TC1 sheets after unidirectional and cross rolling are listed in Table 1 . The results show that transverse yield strength exceeds rolling direction yield strength for both unidirectional and cross rolled sheets, while differences in ultimate tensile strength and elongation between the two directions are minimal.

Table 2 presents room temperature tensile properties along RD and TD after annealing at 750 °C for 30 min and air cooling. After annealing, the sheets retain anisotropy, with transverse yield strength remaining higher than rolling direction yield strength for both processes, and minimal differences in ultimate tensile strength and elongation between directions. Comparing the two rolling methods, unidirectional rolling shows slightly higher elongation after annealing within experimental error, with other properties similar to cross rolling.

Discussion

3.1 Effect of Rolling Deformation on Microstructure

During cooling from the β phase field after PAM, TC1 alloy undergoes $\beta \rightarrow \alpha$ transformation, forming Widmanstätten structure (Figure 2). During breakdown rolling, deformation begins at the transus temperature; when temperature decreases to the two-phase region, the α phase undergoes heavy deformation, refining the microstructure (Figure 3). After breakdown rolling, both α colony size and lamellae thickness are significantly refined, thereby improving alloy ductility and enhancing subsequent workability.

Previous studies have investigated the effects of unidirectional versus cross rolling on titanium alloy microstructure. Song et al. found that for TC4 alloy, directionality of elongated α phase is more severe under unidirectional rolling than cross rolling. Zheng and Lei studied TC4 alloy processed by single cross rolling versus non-cross rolling, finding that non-cross rolling produced predominantly lamellar structure with only small amounts of equiaxed α, while single cross rolling homogenized the microstructure and improved lamellar structure. Gurao et al. investigated microstructure of a β titanium alloy under unidirectional and multi-pass cross rolling, concluding that both processes produce flow lines; in unidirectional rolling, flow lines are essentially parallel to the rolling direction, while in multi-pass cross rolling, flow lines from the two directions appear in a cross-hatched pattern.

In this study, after breakdown rolling and subsequent rolling deformation (both unidirectional and cross rolling), α lamellae undergo distortion and fragmentation under local shear stress (Figure 4). The rolling plane after unidirectional rolling shows deformation α phase clearly aligned along the rolling direction (Figure 4a). Due to different stress histories in α phase during different rolling modes, cross rolling produces less pronounced alignment of α phase along the rolling direction (Figure 4c). Both processes show microstructures aligned along the deformation direction on longitudinal sections (Figures 4b and d), consistent with literature results.

Although the rolling temperature in this study was above the recrystallization temperature, the high deformation rate prevented complete recrystallization in TC1 alloy, thus retaining substantial deformed microstructure. During subsequent static recrystallization annealing, the deformed lamellar α phase spheroidized and grew (Figure 5).

3.2 Effect of Rolling Deformation on Texture

During rolling, plastic deformation dominated by dislocation motion and dynamic recrystallization involving recovery, nucleation, and grain growth occur simultaneously or alternately, influencing both the intensity and type of deformation texture. According to Philippe et al., the deviation of (0002) plane normals toward TD results from coordinated activation of { MATH_{16} } slip, { MATH_{17} } tensile twinning, and { MATH_{18} } compressive twinning. Therefore, after breakdown rolling in this study, the α-phase (0002) plane normals show significant deviation toward TD (Figure 6a). Considering that the breakdown temperature was at the β transus temperature with no intermediate reheating between passes, relatively strong β deformation texture and dislocation substructures likely enhanced the orientation selection process during $\beta \rightarrow \alpha$ transformation, resulting in very strong TD texture components (Figure 6a). The texture component deviating 45° from RD and TD arises from orientation selection during $\beta \rightarrow \alpha$ transformation when breakdown rolling occurs at the phase transformation temperature.

Generally, TC series titanium alloys rolled in the low-temperature region of the $\alpha+\beta$ two-phase field exhibit mixed prismatic and basal texture types, where {0002} plane normals are parallel to both TD and ND directions. Singh and Schwarzer further demonstrated that multi-pass cross rolling causes deviation of {0002} plane normals from ND toward RD. However, in this study, sheets processed by either unidirectional or cross rolling show texture dominated by prismatic texture with mixed basal texture characteristics, with {0002} texture showing no significant deviation toward RD (Figure 7). This occurs because the number of cross rolling passes was limited, so the sheets primarily exhibit unidirectional rolling texture characteristics. Nevertheless, different rolling modes still resulted in weaker texture intensity for cross rolling compared to unidirectional rolling.

3.3 Effect of Rolling Deformation on Room Temperature Properties

Room temperature properties of rolled sheets are primarily influenced by microstructure and texture. In this study, the two rolling processes produced similar microstructural morphologies, resulting in minimal differences in room temperature properties (Table 1). However, for both unidirectional and cross rolling, yield strength along TD is greater than along RD. For titanium alloys at room temperature, the critical resolved shear stress for prismatic slip is much lower than for other slip mechanisms. With prismatic texture present in both rolling processes, when the stress axis is along RD, the angle between the c-axis and stress axis approaches 90°, making prismatic slip the most easily activated deformation mechanism. When the stress axis is along TD, the angle between c-axis and stress axis is small, making prismatic slip difficult to activate, and deformation occurs primarily through more difficult basal or <a+c> slip, resulting in pronounced yield strength anisotropy.

Texture significantly affects yield strength but has minimal influence on ultimate tensile strength, consistent with Zhu et al.'s findings on texture effects in pure titanium. After annealing at 750 °C, α phase spheroidized in sheets produced by both processes (Figure 5), with similar microstructures and properties characterized by improved ductility and reduced yield and ultimate tensile strengths. For titanium alloys, annealing does not significantly alter texture type; therefore, transverse yield strength remains higher than rolling direction yield strength after annealing.

Conclusions

1. The as-cast microstructure of plasma cold hearth melted ingots exhibits Widmanstätten structure. After breakdown rolling at the β transus temperature, the microstructure transforms to β-processed structure with reduced α colony size and α lamellae thickness. Subsequent rolling in the $\alpha+\beta$ two-phase region using both deformation processes distorts, fragments, and realigns α colonies. Unidirectional rolling produces more pronounced alignment of deformation α phase along the rolling direction compared to cross rolling.

2. After breakdown rolling at the β transus temperature, the sheet exhibits primarily prismatic texture. Following $\alpha+\beta$ two-phase region rolling, sheets produced by both processes show mixed texture characteristics dominated by prismatic texture with basal texture components, with cross rolling producing weaker texture intensity than unidirectional rolling.

3. Sheets produced by both rolling processes exhibit higher transverse yield strength than rolling direction yield strength, with similar ultimate tensile strength and elongation. After annealing, sheet strength decreases while elongation increases, and transverse yield strength remains higher than rolling direction yield strength.

References

[1] Mo W. Titanium. Beijing: Metallurgical Industry Press, 2008: 330
[2] Ma JM, He JY, Pang KC. Ingot and Forging of Titanium. Beijing: Metallurgical Industry Press, 2012: 82
[3] Chinnis WR. Titanium 1990: Products and Application, 1990; 2: 830
[4] Tian YX, Li SJ, Hao YL, Yang R. Acta Metall Sin, 2012; 48: 837
[5] Zhang ZQ, Dong LM, Yang Y, Guan SX, Liu YY. Acta Metall Sin, 2011; 47: 1257
[6] Wang T, Guo H, Wang Y, Yao Z. Mater Sci Eng, 2010; A528: 736
[7] Ding R, Guo ZX, Wilson A. Mater Sci Eng, 2002; A327: 233
[8] Lütjering G. Mater Sci Eng, 1998; A243: 32
[9] Roy S, Karanth S, Suwas S. Metall Mater Trans, 2013; 44A: 3322
[10] Gurao NP, Ali AA, Suwas S. Mater Sci Eng, 2009; A504: 24
[11] You L, Song XP. Acta Metall Sin, 2008; 44: 1310

[12] Qin GH, Wang WB, Ji B, Wu YY. Chin J Nonferrous Met, 2010; 20: 877
[13] Song JH, Hong KJ, Ha TK, Jeong HT. Mater Sci Eng, 2007; A 449–451: 144
[14] Zheng JM, Lei RQ. Titanium Industry Progress, 2008; 25(4): 27
[15] Boehlert CJ. Mater Sci Eng, 2000; A279: 118
[16] Mao WM, Yang P, Chen L. Analysis Principle of Texture and Testing Technique. Beijing: Metallurgical Industry Press, 2008: 15
[17] Philippe MJ, Esling C, Hocheid B. Textures Microstruct, 1988; 7: 265
[18] Salem AA, Glavicic MG, Semiatin SL. Mater Sci Eng, 2008; A496: 169
[19] Warwick JLW, Jones NG, Bantounas I, Preuss M, Dye D. Acta Mater, 2013, 61: 1603
[20] Singh AK, Schwarzer RA. Mater Sci Eng, 2001; A307: 151
[21] Gey N, Humbert M, Philippe MJ, Combres Y. Mater Sci Eng, 1996; A219: 80
[22] Russell AM, Chumbley LS, Ellis TW, Laabs FC, Norris B, Donizetti GE. J Mater Sci, 1995; 30: 4249
[23] Zhu ZS, Gu JL, Chen Nan P. Chin J Nonferrous Met, 1995; 5: 83
[24] Zhu ZS, Gu JL, Chen Nan P, Yang ZS. Mater Mech Eng, 1994; 18: 23
[25] Lin P, Feng A, Yuan S, Li G, Shen J. Mater Sci Eng, 2013; A563: 16